Self-healing capability of concrete with crystalline admixtures in different environments

M. Roig-Flores [a,*], S. Moscato [b], P. Serna [a], L. Ferrara [b]

[a] *ICITECH-Institute of Concrete Science and Technology, Universitat Politècnica de València, Valencia, Spain*
[b] *Politecnico di Milano, Milano, Italy*

1. Introduction

Self-healing materials are those which have the capability of autonomously repairing small damages or cracks. The main reason for investigating the properties of self-repairing materials is that constructions built with them will have increased their service-life; likewise, structures with difficult or expensive repara-tions will benefit from self-healing their own damages [1]. Thus, self-healing concrete will lead to an increase of the sustainability of the structures built with this material.

Concrete has an inherent healing potential, called autogenous healing, which can take place in ordinary concrete elements but its power is limited and is not predictable. Neville in 1981 already mentioned this phenomenon and proposed the causes to autogenous healing [2]. He found out that fine cracks may heal completely under moist conditions and explained this phenomenon

* Corresponding author at: ICITECH-Institute of Concrete Science and Technol-ogy, Universitat Politècnica de València, 4N Building, Camino de Vera s/n, 46022 Valencia, Spain. Tel.: +34 963877563x75631.
E-mail addresses: marroifl@upv.es (M. Roig-Flores), simone.moscato@gmail.com (S. Moscato), pserna@cst.upv.es (P. Serna), liberato.ferrara@polimi.it (L. Ferrara).

by both the delayed hydration of unhydrated cement and carbonation. Later, those processes were studied by Hearn (1998), Edvarsen (1999) and ter Heide (2005): all the authors agreed that the main processes responsible of self-healing were delayed hydra-tion for young concrete while carbonation was more relevant for older elements [3–5]. Recent studies have compared the use of cement with different percentages of Portland cement and addi-tions in the autogenous healing process, obtaining better results with cements containing blast furnace slag or fly ash, which enhance the effect of delayed hydration, while carbonation precip-itation remains similar for the different binder types [6–8]. Other studies were focused on the use of fibers in order to restrict crack width and enhance autogenous healing [9,10], using different fibers made of different materials [11] and analyzing the healing process under different environmental exposures [12].

In any case, autogenous healing is not a reliable phenomenon in order to get significant healing effects. That is the reason why several new "engineered healing concepts" have been investigated in the last years, such as the use of microencapsulated healing agents [13,14], bacterial concrete [15] or the use of crystalline admixtures [16].

Crystalline admixtures (CA) are a special type of permeability reducer admixtures (PRAs) as reported by the ACI Committee 212 [17]. In contrast to water-repellent or hydrophobic products, these materials are hydrophilic, and this makes them to react easily with water. When this reaction takes place, it forms water insoluble pore/crack blocking deposits that increase the density of Calcium Silicate Hydrate (CSH) and the resistance to water pene-tration. In this case, the matrix component which reacts is the tri-calcium silicate (C_3S) and water presence is also needed. These products are formed by active chemicals contained in cement and sand which form modified CSH, depending on the crystalline promoter, and a precipitate formed from calcium and water mole-cules. Crystalline deposits become part of the matrix, unlike hydrophobic materials, thus being able to resist pressures as high as 14 bars [17].

Some authors studied the visual closure produced by different additives in mortar specimens comparing with a reference Portland mortar using fly ash, expansive admixtures, silica fume, crystalline admixtures and limestone powder with complete water immersion as healing exposure [18]. It was shown that crystalline admixtures improved self-healing processes at a higher rate than other types of additions, in the range of small cracks (less than 0.05 mm); however, they became inefficient for wider cracks. In other studies, the self-healing measured by means of the evolution of the permeability and visual closure was studied, comparing the effect of crystalline admixtures, expansive admixtures and a combination of both products. The limits were shown of the self-healing capability of crystalline admixture for cracks wider than 150 μm, while the combination of both agents achieved complete self-healing for cracks up to 400 μm after 30 days of water immer-sion [16]. Regarding the recovery of mechanical properties, study-ing ordinary concrete and high performance fiber-reinforced concrete with crystalline admixtures, a better self-healing response was found for some parameters, such as the recovery of strength [19]. Other authors analyzed the healing effect of those admixtures under four different exposures (water immersion with/without renovation, wet/dry cycles, humidity chamber or air exposure) in terms of recovery of strength, obtaining the best results for the water immersion [19] or the wet/dry exposure [20].

The study of self-healing properties is based on the controlled creation of a specific damage (e.g. cracks) and the evolution of that damage under different conditions, which could be depicted by mechanical or durability properties. In recent years different pro-cedures have been published to this purpose. Several methodolo-gies have been proposed in order to analyze the permeability of cracked specimens, either simultaneously with the performance of load tests [21] or using independent tests for each phase [16]. In regards to the relation between the induced damage and the permeability properties, Edvardsen proposed a cubic relation between the water flow passing through a cracked concrete speci-men and the crack width with an expression derived from Poiseuille Law [4].

2. Research objectives

The main objectives of this research can be summarized as follows:

- To analyze the effect of crystalline admixtures with reference to the enhancement of self-healing mechanisms.
- To determine the influence of the environmental exposure in self-healing of concrete with and without crystalline admixtures.
- To develop and compare methods for evaluating the self-healing properties of cracked specimens, based on the measure of the global permeability of the specimen and different geo-metrical characteristics of the crack before and after the self-healing period.

3. Experimental program and materials

3.1. Experimental program

In this study, it was decided to maintain the crack width always below 0.3 mm, as it is a common threshold for crack width in service state and it is potentially seal-able by autogenous and CA healing, according to the available literature. The age of pre-cracking was fixed at 2 days, as most of the cracks due to shrinkage may occur few days after casting time. The initial permeability test was performed 1 day after pre-cracking, because of the needs related to the experimental procedure. Finally the time set for the self-healing process before the last permeability evaluation was 42 days; as a matter of fact, in most studies specimens got sealed in a shorter period of time when exposed to water immersion.

The experimental variables which were studied in this research are:

- Crystalline admixture dosage: 0% (control specimens), 4% by the weight of cement (CA specimens).
- Self-healing exposure: water immersion (WI), water contact (WC), humidity chamber (HC) and air exposure at laboratory conditions (AE).

This study includes both a main study of permeability evolution and an analysis about the methodology for image evaluation of the crack. A total of eight groups of specimens were cast for permeability tests, each consisting of six concrete speci-mens. Additional specimens were cast for some groups that required further explo-ration. Among all the specimens: three per each group were also employed for image evaluation of crack parameters. An overview of the final number of cast speci-mens for each group is summarized in Table 1: as a whole 61 specimens were tested for permeability whereas image analysis of the cracks was performed on 24 specimens.

3.2. Materials and mixture proportions

It was decided in this study to work with fiber-reinforced concrete. Since the focus of the project was to study the healing effects on pre-cracked specimens, fibers could provide an effective action both in controlling crack width during the pre-cracking process as well as in keeping fixed its value afterwards. The quantity of steel fiber was fixed at 40 kg/m^3 according to the criterion of making the crack opening easily controllable while avoiding excessive branching of cracks.

The cement used was CEM II/A-L 42.5 R from Elite Cementos S. L. The water/ce-ment ratio used was 0.45 in both types of concrete. A dosage of 4% by the weight of cement of crystalline admixture in powder form was introduced in the CA Concrete whose behavior was compared with control specimens (without crystalline admix-ture). The two mix designs are shown in Table 2.

The criterion chosen for making concrete mixes with and without crystalline admixture is to maintain constant the sum of limestone powder and crystalline admixture, due to their similar effect on concrete workability. As a matter of fact they would both act as densifiers of the paste matrix phase. Superplasticizer, ViscoCrete 5720, dosage was adjusted in each different group in order to get similar slump (140 mm ± 20 mm).

Table 1
Number of specimens cast for each group.

Concrete	Exposure conditions	Number of specimens for permeability tests	Number of specimens for image analysis tests
Control	Water immersion	6	3
	Water contact	7	3
	Humidity chamber	8	3
	Laboratory conditions	9	3
CA	Water immersion	8	3
	Water contact	8	3
	Humidity chamber	8	3
	Laboratory conditions	7	3

Table 2
Mix design of control and CA concrete.

Material (kg/m^3)	Control	CA Concrete
Cement II/A-L 42.5 R	350	350
Water	157.5	157.5
Gravel (4–12 mm)	950	959
Natural sand	899	875
Fibers, Dramix 65/35	40	40
Limestone powder (LP)	50	36
Crystalline admixture (CA)	–	14
Additional fine fraction: LP + CA	50	50
Average slump (cm)	13	15
Average compressive strength (MPa)	53	61

In total, 7 batches of control concrete and 6 of crystalline admixture concrete were cast. For each batch, three $\Phi 150 \times 300$ mm cylindrical specimens were cast according to UNE-EN 12390-2 to determine the compressive strength at 28 days, as per UNE EN 12390-3. All batches were also characterized by their workability with slump test as per UNE EN 12350-2:2009. These control tests were performed with the objective of verifying the homogeneity of specimens of different batches but belonging to a same mix group (either control or CA) and in order to compare the results between the two mix groups (control and CA). After averaging the results of all batches for each group, it was observed that CA concrete had a significantly better compressive strength, about 15% higher than control concrete. With reference to the slump test results, differences are slightly lower, since the average results are around 13 cm for control concrete and 15 cm for CA concrete, which are within the acceptable tolerance limits of slump tests according to the standards.

4. Experimental methodology

The methodology used in this research to evaluate the effects of self-healing consists of four stages: first, the creation of controlled damage in the specimens; second, the measure of the recovery of certain properties; third, the simulation of the conditions or environmental exposure needed to achieve better healing results and, finally, the evaluation of the recovery of the same property measured in the second stage. The self-healing effect has been checked by analyzing the concrete permeability of cracked specimens before and after the self-healing process and with the evolution of geometrical parameters of cracks, namely its width and/or area.

4.1. Creation of a damage: pre-cracking process

Cylindrical specimens ($\Phi 150 \times 150$ mm) were pre-cracked at the age of 2 days, inducing, by means of a splitting test, a controlled damage (Fig. 1): this was meant as the width of the crack, which

was set to reach a target value, controlled by a calibration ruler. The measure of the crack width with the calibration ruler while performing the splitting test has been meant as good enough to obtain crack widths within a range of 0–0.3 mm.

4.2. Evaluation of properties: permeability test

A method based on the permeability test described in UNE-EN 12390-8 was employed in this study, but measuring the water flow instead of the water depth penetration. To guarantee the impermeability of the specimen lateral surface, the zones of the lateral surface which were in contact with the machine loading platens during the pre-crack splitting tests were sealed with an epoxy resin Sikadur 31-CF as shown in Fig. 2. It should be noted that resin does not enter significantly inside the crack, since it is only placed externally.

The test was performed by applying a head water pressure equal to 2.00 ± 0.05 bars. The quantity of water passing through the crack was measured during a 5 min testing time. This proce-dure results in higher water flows for larger crack widths. In this way, if a crack closes after the healing process, the water flow should have been diminished. The permeabilimeter used in the test and the different parts it consists of it are shown in Fig. 3.

4.3. Evaluation of properties: study of crack geometrical parameters

In addition, crack geometry parameters were also measured to support measurements from permeability tests. The

Fig. 1. Pre-cracking process of a concrete specimen.
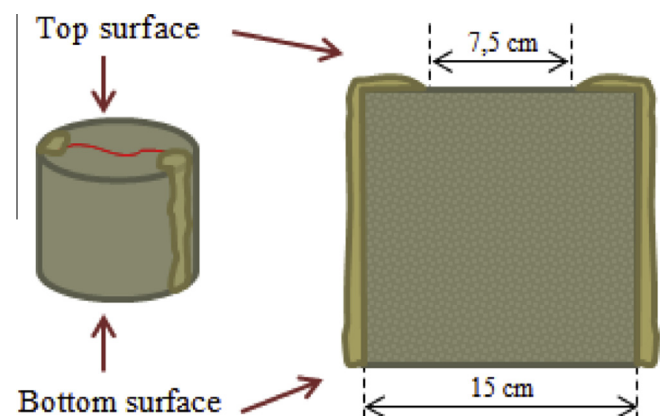
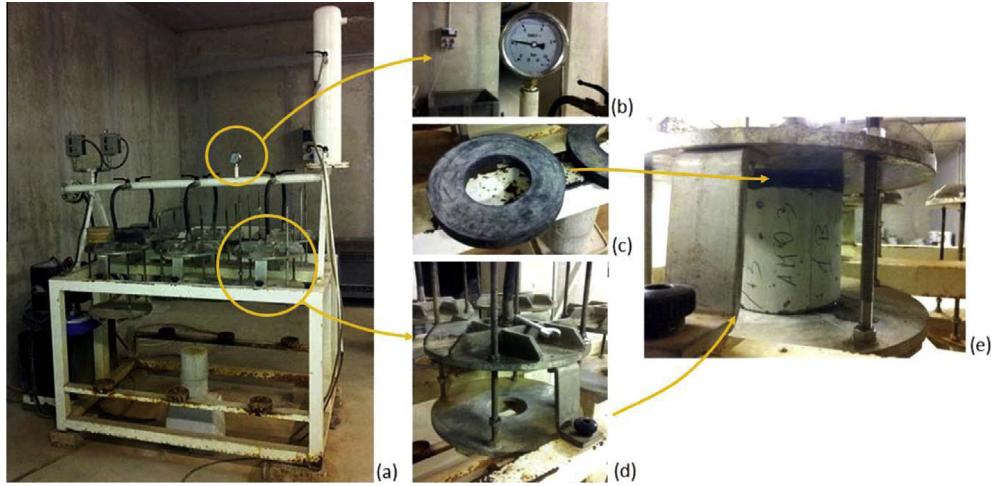**Fig. 2.** Lateral sealing of specimens with Sikadur.

Fig. 3. Permeabilimeter (a) and its parts: manometer (b), sealing ring (c), auxiliary structure (d), prepared specimen (e).

measurements are based on the study of composed panorama pictures showing the cracks all along their length; the photography software Adobe Photoshop CS6 was used for image processing. Each single picture was of size 1600×1200 pixels, covering an area of 8×6 mm, therefore 1 pixel was equivalent to 5 μm. The resolution of the images was maintained in the bigger panorama images, thus 5 μm was the limit of resolution of the measurements. These pictures were taken before and after the healing exposure, with a digital optical microscope ($\times 60$, $\times 200$). Before taking pictures all the specimens were cleaned with compressed air.

The measurement of crack geometrical parameter has been performed with a twofold purpose: first, to seek a correlation with the water flow measured in the permeability tests; and, second, to analyze the significance of the evolution of the same geometrical parameters as indicators of self-healing. To this twofold purpose, the ratios between final and initial values of the water flow and of crack geometrical parameters were calculated. Water permeability is considered the reference value in order to compare the different methods for quantifying self-healing, since the main objective of closing a crack is to avoid the entrance of liquids, contaminants and aggressive agents.

Crack geometrical parameters can be divided in two groups: the measure of crack width and the measure of crack area. Crack area was expected to be a better indicator of the physical closing, because it would include the crack width all along the whole length of the crack. Four crack geometrical parameters have been measured in this research:

- w_{max}, maximum crack width: by means of graphic software, the maximum crack width along the whole crack length is determined, in millimeters.
- w_{avg}, average crack width: by means of graphic software, crack width (in millimeters) is determined in five fixed positions and averaged.

- A_{est}, estimated from average crack width w_{avg}: using the five measures of crack width and multiplying by their associated lengths, in squared millimeters.
- A_{px}, measuring black pixels: by using graphic software, black pixels in the image are counted, which indicate crack area.

The average width w_{avg} was calculated averaging five width measurements, taken at prescribed positions along the crack. A grid was prepared to overlap on the panorama pictures, after bringing the grid at the same scale of the picture (Fig. 4). Specifically, two grids were used, one for the top cracks and the other for the bottom cracks, because of the different crack length in each surface (7.5 cm in the top crack and 15 cm in the bottom).

The second group consists of the measurement of an averaged crack area and the measure of black pixels in an image. By means of the same approach used to calculate w_{avg}, the area of the cracks is estimated by multiplying the five measured widths, in millimeters, by their associated lengths obtaining the area in squared millimeters A_{est}. In this way, the resulting area is approximated as the sum of the areas of five rectangles. The second method to calculate the area of the cracks involves the use of the graphical software to quantify the number of black pixels inside the pictures. In order to avoid that pores or other dark parts of the pictures affect the quantification of black pixels, all the panoramas were cleaned by a specific tool of the software (Fig. 5).

4.4. Exposure simulation

Four environmental exposures were studied in order to determine the effect of humidity on the self-healing capability of the tested specimens, comparing the reference concrete with the crystalline admixture concrete (Fig. 6).

(a) WI (water immersion): continuous immersion in tap water at laboratory conditions without renewing the water during the healing period (temperature of water, 15–16 °C).
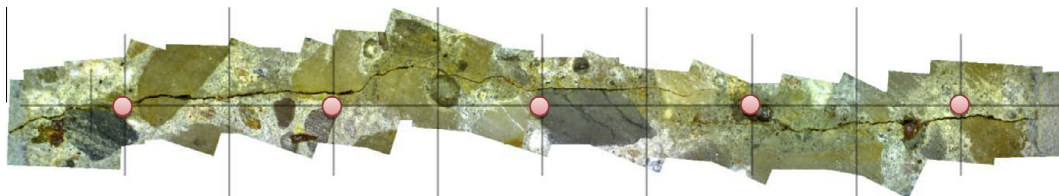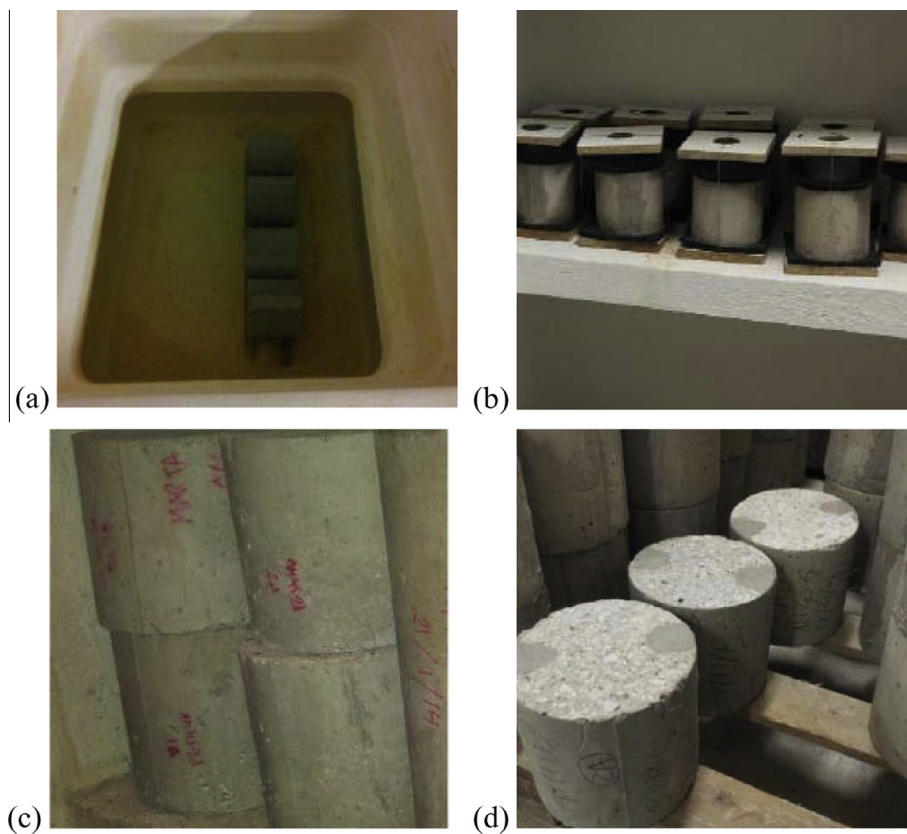

Fig. 4. Panorama of a top crack and grid marking the measuring points.

Fig. 5. Panorama of a top crack and its black pixels (before cleaning).

Fig. 6. Four exposures: water immersion (a), water contact (b), humidity chamber (c) and air exposure (d).

(b) WC (water contact): a layer of water with a head pressure of 2 cm-water on the top crack, and storage in humidity chamber at 20 °C and 95 ± 5% relative humidity. Additional water was supplied when necessary in order to maintain the 2 cm water layer.

(c) HC (humidity chamber): storage of the specimens inside a standard humidity chamber at 20 °C and 95 ± 5% relative humidity.

(d) AE (air exposure): storage of the specimens in normal laboratory conditions inside a room without exterior influences (17 °C and 40% RH).

Each type of healing exposure has been designed with the objective of simulating practical conditions. WI simulates underwater concrete elements; WC simulates situations with a face directly exposed to water with a very low pressure and the other unexposed to it, such as buried walls under the water table; HC simulates concrete elements without direct contact with water but constructed in a high humidity environment and AE concrete elements without direct contact with water and average humidity levels. With these four environmental conditions, it is intended to discern if the self-healing will be powerful enough for constructions in several types of environments as above.

The specimens immersed in water during the healing period, were divided in two different water recipients, in order to avoid interferences between control concrete and concrete with crystalline admixtures. The setup for the 2 cm water contact environment is shown in Fig. 7. In this group, water remains in the
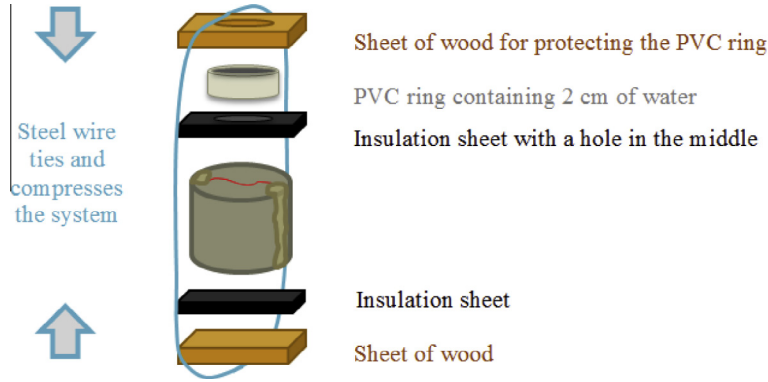
Fig. 7. Setup of the 2 cm water head exposure.

upper PVC ring and enters inside the specimen through the crack and does not exit from it because of the lower sheets of insulation and wood.

5. Results and discussion

5.1. Morphology of healed cracks

As a first and most immediate aspect of the occurred crack sealing, it might be worth noticing the whitish formations in control and CA specimens when immersed in water, which can be clearly seen in Fig. 8. For specimens conditioned in the "water contact" environment, those white precipitates were only formed on the face in direct contact with water. This fact indicates that the transportation of water through the crack with a water head of 2 cm is not enough for ensuring healing of both faces.

The formations were located all along the surface of the specimens in contact with water (for WI and WC exposures), not only inside the crack, and were frequently accumulated also in some pores. In some cases, the precipitates were slightly yellowish, which is supposed to be originated by the oxidation of steel fibers, but the analysis of this effect was beyond the scope of this work.

Another interesting aspect that could be studied through the analysis of the complete crack pattern panoramas is determining whether the healing occurred only when the crack was in the cement paste or if it also occurred when the crack broke through an aggregate or in the paste-aggregate interface. In the specimens with sealed or almost sealed cracks this aspect was analyzed, and it was concluded that most formations were originated in the cement paste: this is expected, because crystalline admixture is dispersed in concrete matrix among with the cement particles. Anyway, it was also powerful enough to transport the healing products inside small cracked aggregates, which is an indicator of the effectiveness of the self-healing agent.

5.2. Self-healing results: water flow vs. crack geometry parameters

When representing water flow versus the four crack geometry parameters obtained from image analysis, it has to be observed that the best correlations were obtained from the relation between water flow and the $A_{mm}{}^2$ (Fig. 9c) and with the averaged crack width w_{avg} (Fig. 9a). The chosen trend lines are cubic functions depending on the crack geometry parameter: as explained from the literature, the water flow in a cracked specimen depends on the third order power of the crack width [7]. On the other hand, the correlation between water flow and w_{max} (Fig. 9a) and A_{px} (Fig. 9d) were highly dispersed and therefore these crack geometry parameters are proved to be worse indicators of the level of damage of the cracked specimens and the resulting self-healing.
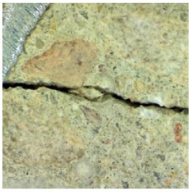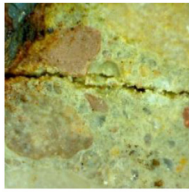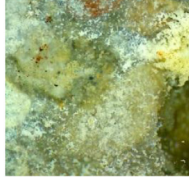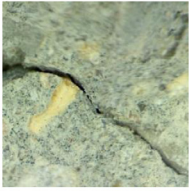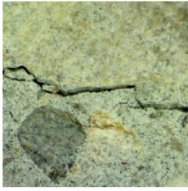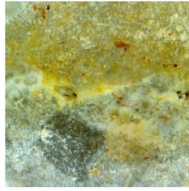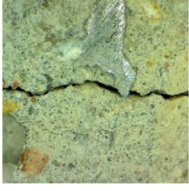
As a matter of fact, it can be observed that the measure of black pixels achieved the worst results. There are two possible reasons for this behavior: (a) the three-dimensional effect of the interior part of cracks, which makes crack pixels turn gray in the photographs while still being part of the crack; and (b) the small interferences of black pixels outside the crack, though they were cleaned for minimizing this effect.

For the two best methods, polynomial cubic trend lines were calculated by applying the boundary conditions of zero flow in correspondence of zero damage and horizontal tangent at zero flow. Adjusted R-squared (R_{adj}^2) was used in order to evaluate the goodness of fit of the model.

It may be important to remark that in each specimen two cracks were formed, on the top and the bottom surface. When choosing the value of the crack geometry parameter in order to study its relation with water flow, several options could be considered: the value of the parameter for the top/bottom crack, the minimum or the maximum, the average value, etc. The minimum crack and the averaged crack were expected to be the best parameters in order to represent the damage comparing with the permeability results, the first option because the minimum section may restrict water flow and the latter because it is an estimation of the 3D vol-ume of the crack considering it as a pyramidal frustum. The results in Fig. 9 were represented using the averaged result from both top and bottom surface cracks. Other relations were also analyzed and they showed notably worse results for the cases of choosing the minimum, and maximum value of cracks, for one of the best parameters, $A_{mm}{}^2$. Choosing the top or the bottom crack as parameter did not showed any stable trend. Very similar results were achieved when analyzing the averaged crack width parameter w_{avg}.

The results of the relationship between the obtained ratios of final and initial water flow and the ratios from the final and initial values of the crack geometry parameters (averaged from the top and bottom cracks for each specimen) can be seen in the graphs in Fig. 10. As expected higher water flow ratios correspond to higher crack geometry parameter ratios. Control specimens got significantly high dispersion while CA group showed a highly linear behavior for both methodologies of evaluating the crack geometry.

The dispersion obtained in the results of this research could be caused by self-healing taking place inside a crack but not on the surface of the specimen, where the crack parameters have been measured, as crystallization could start easily in the zones with smaller crack width. Fig. 11 represents a simplification of some of the possible interior morphologies of a crack in a concrete specimen, and the points that might be more suitable in order to start

		Control concrete		Concrete with Crystalline Admixtures	
		Before healing	**After healing**	**Before healing**	**After healing**
EXPOSURE	Water Immersion		Crack closure ~ 75%		Crack closure ~ 100%
	Water Contact		Crack closure ~ 60%		Crack closure ~ 100%
	Humidity Chamber		Crack closure ~ 0 %		Crack closure ~ 0 %
	Air Exposure		Crack closure ~ 0%		Crack closure ~ 0 %

Fig. 8. Comparison between crack aspect at 0 days and after 42 days of healing, for control and CA specimens exposed to the four environments: water immersion (WI), water contact (WC), humidity chamber (HC) and air exposure (AE).

the precipitation of crack healing products. If the morphology of the crack is a concave volume, the interior of the crack may be healing while the visible crack would stay immutable, which could distort the calculated ratios and affecting the results. Moreover, if crystalline admixtures generate more strongly adhered crystals than those produced in control specimens, it could be possible than the water flow causes a random crystals migration in control concrete; thus producing more variable results in the permeability of control concrete.

5.3. Self-healing results: permeability

The self-healing properties based in the evolution of permeability are evaluated by means of the healing rate, which is defined as

$$\text{Healing rate} = 1 - \frac{\text{Final flow}}{\text{Initial flow}} = 1 - \frac{Q_{42}}{Q_0}$$

With Q_0, the initial water flow; Q_{42}, the final water flow for a healing time of 42 days.

When the final flow is similar to the initial flow, the healing rate would tend to 0; and when the final flow is 0, the healing rate would be 1. Negative values of the healing rate would show a reopening of the crack. The healing produced depending on the initial level of damage can be analyzed by representing the healing rates obtained for each specimen versus its initial water flow.

A more stable self-healing rate was achieved for specimens made with concrete containing the crystalline admixture (CA) than for control specimens, which show high dispersion as the amount of available water is reduced. The specimens immersed in water (Fig. 12a) and in contact with 2 cm of water layer (WC, Fig. 12b) achieved higher healing rates (between 0.75 and 1). The exposure which showed the best healing behavior was water immersion, in which crystalline admixture specimens showed slightly better behavior than the control group. For specimens in WC exposure there is a clear overlapping between the control and CA groups. The specimens stored in humidity chamber (Fig. 12c) and in laboratory conditions (Fig. 12d) showed lower results, with healing rate values generally lower than 0.5 even reaching negative values of healing rate.

The results classified depending on the type of mixture, are shown in Fig. 13a (for control concrete) and Fig. 13b (for CA concrete). In the case of control specimens (Fig. 13a), the results show a high dispersion. However, a clear tendency of better healing rates when increasing the available water can be observed. Moreover, no notable differences were observed between the specimens immersed in water immersion and those in water contact conditions. On the other hand, for CA concrete (Fig. 13b), the results can be clearly gathered in two groups: those in direct contact with water, either immersed or with a moderate head pressure, and those exposed to air humidity, either controlled or natural. Again,
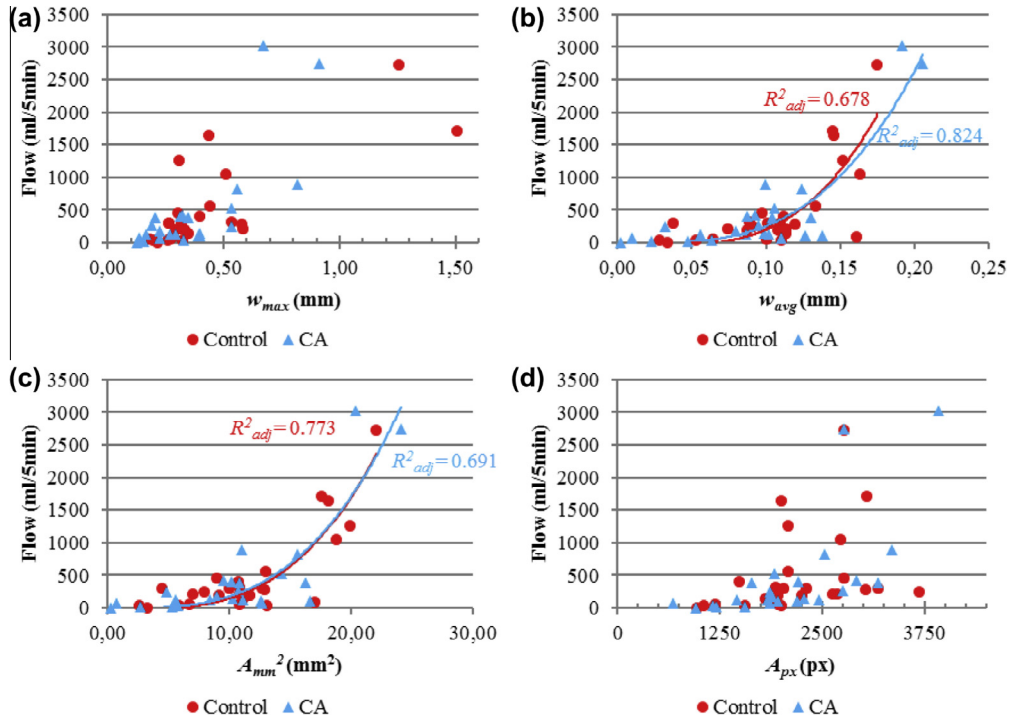
Fig. 9. Relation between water flow and the geometrical parameters: (a) maximum crack width w_{max}, (b) averaged crack width w_{avg}, (c) estimated crack area A_{mm}^2, (d) amount of black pixels A_{px}.
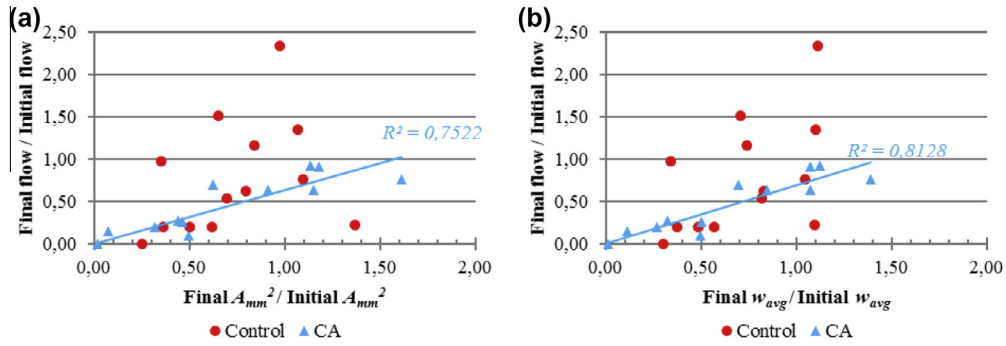
Fig. 10. Relation between water flowratio and estimated crack area A_{mm}^2 ratio (a) and water flow ratio and averaged crack width w_{avg} ratio (b).
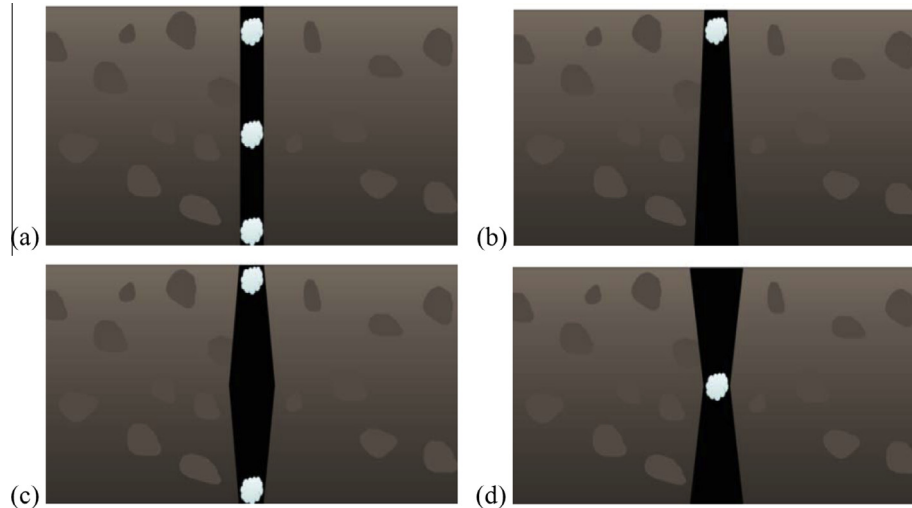
Fig. 11. Simplification of different possibilities for crack geometry in depth: uniform crack, pyramidal frustum, convex and concave forms and their most feasible points for precipitates.
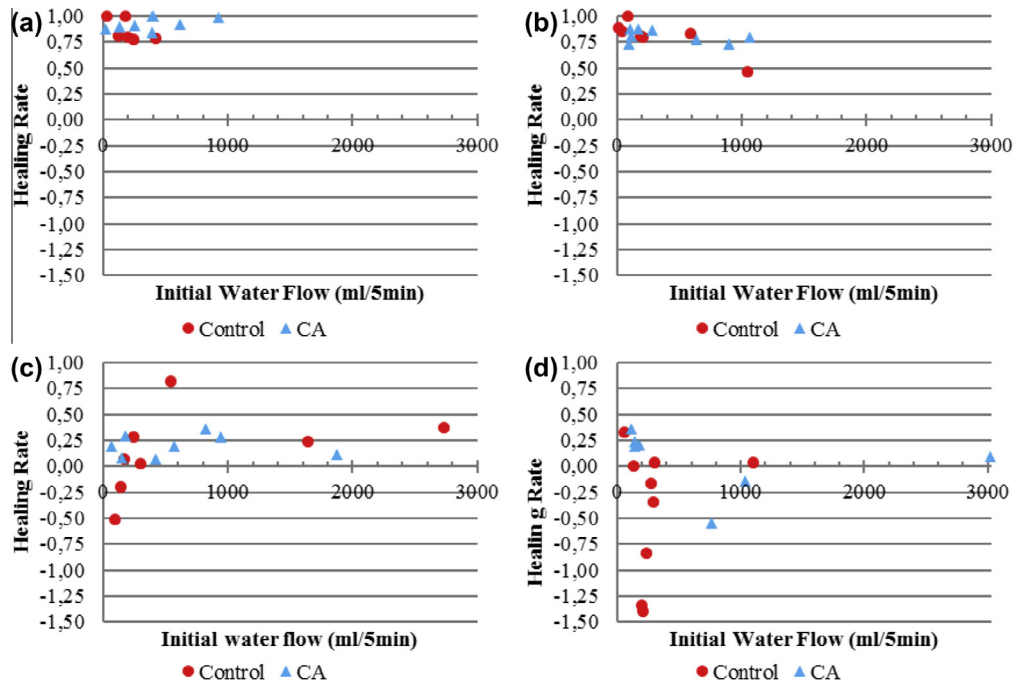
Fig. 12. Control and CA concrete in the four exposures: water immersion (a), water contact (b), humidity chamber (c) and air exposure (d).
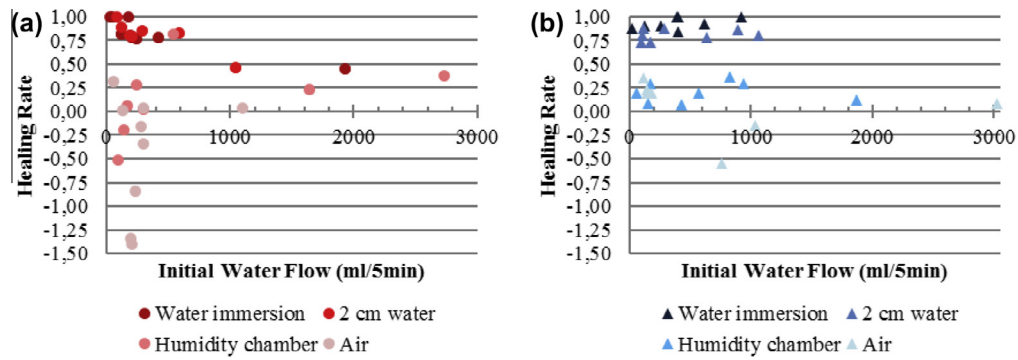

Fig. 13. Behaviour of control concrete (a) and CA concrete (b) for the four different exposures.

the more water available for the specimen, the higher healing rate is achieved. In the case of crystalline admixtures concrete, the results are clearly concentrated around the average values of 0.93 for WI, 0.81 for WC; 0.21 for HC and 0.17 for AE.

Fig. 14 shows the averaged the results of healing rates for the specimens with an initial water flow lower than 1000 mm per 5 min. The groups with higher healing rates are water immersion (WI) and water contact (WC). Specimens in humidity chamber showed a slightly better result with CA than for control concrete, but there is a significant difference with the previous groups. It can be hence argued that natural environmental humidity is not enough for complete self-healing to take place, even when using CA.

The differences between control and CA specimens when exposed to an environment with a lower humidity could be likely due to drying shrinkage, as in humidity chamber (HC) the water loss would be compensated, but not in the laboratory conditions (AE). In this case, the CA would act as a shrinkage compensator and the cracks, even if not healed, would at least be kept from growing.
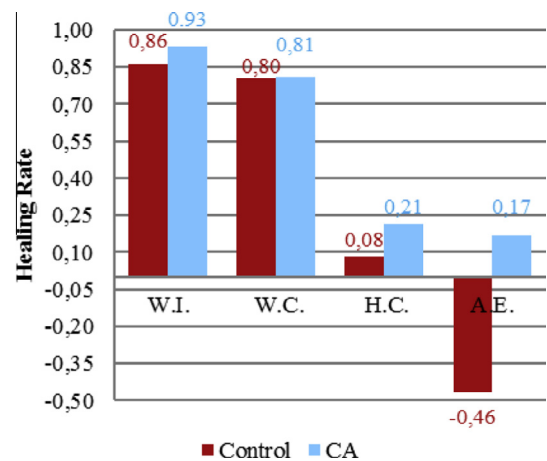

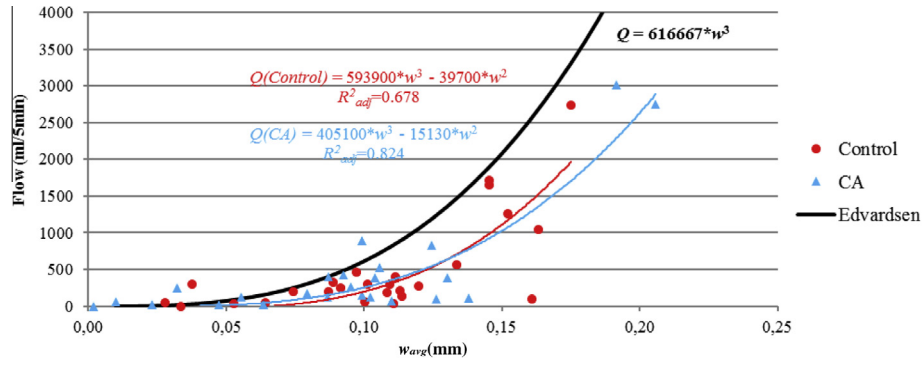Fig. 14. Averaged healing rate for each group.

Fig. 15. Comparison between experimental and theoretical water flow and crack width results.

5.4. Discussion

Edvardsen proposed a model based on Poiseuille Law [4], which is expressed in Eq. (1), for water at 20 °C, viscosity $v = \eta/\rho = 1.00$ mm^2/s and a visible crack length of 1 m; where q_0 is the water flow per meter length of crack, I is the hydraulic gradient in meters of water head per meter, w_{avg} is the mean value of crack width and k_t is a correcting parameter for temperature:

$$q_0 \left(\frac{\text{liters}}{\text{m}} \right) = 740 * I * w_{avg}^3 * k_t \qquad (1)$$

This expression can be adjusted to the parameters of the present research by changing units and the length of the crack (considered as 75 mm), resulting in the expression (2):

$$Q(\text{liters}) = 740 * \frac{20}{0.15} * w_{avg}^3 * 1 * 0.075 \qquad (2)$$

The obtained experimental results of water flow and averaged crack width in this research (shown previously in Fig. 9) fit reasonably well in the theoretical predictions given by Eq. (2) as displayed in Fig. 15. The lower values obtained in this research might be due to the presence of fibers which could help blocking water flow inside the crack.

With reference to the healing rates, similar values have been registered by other authors for permeability properties [16], mechanical parameters or [19,20] closure of crack width [16,18] for specimens under water immersion exposure, with values of effectiveness usually around 90% of recovery, or even higher. The enhancement of effectiveness by crystalline admixtures specimens under water immersion comparing with results of control specimens has been also confirmed by other studies [19], with results similar to those obtained in this work, increasing the healing capability about 7–10% with respect to control concrete. The higher results of specimens from both groups (control and CA) under water immersion WI compared to indoor or air exposure AE specimens obtained in this work are similar to those obtained studying the recovery of mechanical properties in other studies [20].

6. Conclusions

This paper has presented the results of a research comparing different methodologies for quantifying the self-healing capacity of fiber reinforced concrete and the effectiveness of crystalline admixtures as self-healing agent in four different environmental exposures.

The following conclusions can be drawn from the obtained results:

With reference to the test methodology and to the parameters adopted to define and quantify the healing process rate:

(1) Self-healing rate, calculated from the results of the modified permeability test designed in this research, is a reliable indicator of the recovery of durability properties.
(2) The crack geometry parameters evaluated through image analysis have a clear relation with the water flow results when comparing flow with the averaged crack area ($A_{mm}{}^2$) or the averaged crack width (w_{avg}). These parameters can be considered as alternative to water permeability measurement tests. However, as healing indicators, their dispersion is high for control specimens.
(3) Still with reference to crack geometry parameters, the quantification of crack area through measurement of black pixels of a crack panorama was the method with the highest dispersion of the values.

With reference to the influence of concrete composition and exposure conditions:

(4) Specimens with crystalline admixtures showed a more stable and reliable behavior in healing tests, featuring lower dispersion and clearer trends.
(5) Specimens cast with concrete containing crystalline admixtures and stored under water immersion achieved the highest self-healing rates, with values around 0.95 even for the larger initial crack widths (around 0.25 mm) and several specimens with complete healing.
(6) The presence of water is critical for the self-healing to take place for both reference concrete and crystalline admixture concrete. Neither control specimens nor those with crystalline admixtures healed when exposed to moist conditions.
(7) The four exposures in order of decreasing permeability healing rate are: water immersion (around 0.90) > water contact (around 0.80) > humidity chamber (around 0.15) > air exposure (around −0.15).

References

[1] Wua M, Johannesson B, Geiker M. A review: self-healing in cementitious materials and engineered cementitious composite as a self-healing material. Constr Build Mater 2012;28:571–83.
[2] Neville AM. Properties of concrete. 3rd ed. Longman; 1981.
[3] Hearn N. Self-sealing, autogenous healing and continued hydration: what is the difference? Mater Struct/Mater Constr 1998;31:563–7.

[4] Edvardsen C. Water permeability and autogenous healing of cracks in concrete. ACI Mater J 1999:448–54.

[5] Ter Heide N. Crack healing in hydrating concrete [M.Sc. thesis]. Delft University of Technology Faculty of Civil Engineering and Geosciences; 2005.

[6] Van Tittelboom K, Gruyaert E, Rahier H, De Belie N. Influence of mix composition on the extent of autogenous crack healing by continued hydration or calcium carbonate formation. Constr Build Mater 2012;37:349–59.

[7] Qian S, Zhou J, de Rooij MR, Schlangen E, Yea G, van Breugel K. Self-healing behavior of strain hardening cementitious composites incorporating local waste materials. Cement Concr Compos 2009;31:613–21.

[8] Zhang Z, Qian S, Ma H. Investigating mechanical properties and self-healing behavior of micro-cracked ECC with different volume of fly ash. Constr Build Mater 2014;52:17–23.

[9] Qian SZ, Zhou J, Schlangen E. Influence of curing condition and precracking time on the self-healing behavior of engineered cementitious composites. Cement Concr Compos 2010;32:686–93.

[10] Nishiwaki T, Kwon S, Homma D, Yamada M, Mihashi H. Self-healing capability of fiber-reinforced cementitious composites for recovery of watertightness and mechanical properties. Materials 2014;7:2141–54.

[11] Nishiwaki T, Koda M, Yamada M, Mihashi H, Kikuta T. Experimental study on self-healing capability of FRCC using different types of synthetic fibers. J Adv Concr Technol 2012;10:195–206.

[12] Yang Y, Yang EH, Li VC. Autogenous healing of engineered cementitious composites at early age. Cem Concr Res 2011;41:176–83.

[13] Perez G, Jimenez I, Erkizia E, Gaitero JJ, Kaltzakorta I, Guerrero A. Effect of self-healing additions on the development of mechanical strength of cement paste. Chem Mater Res 2013;5:102–5.

[14] Yang Z, Hollar J, He X, Shi X. A self-healing cementitious composite using oil core/silica gel shell microcapsules. Cement Concr Compos 2011;33: 506–12.

[15] Jonkers HM, Schlangen E. Crack repair by concrete-immobilized bacteria. In: Proceedings of the first international conference on self healing materials 2007, Noordwijk aan Zee, The Netherlands 2007; 1:7.

[16] Sisomphon K, Copuroglu O, Koenders EAB. Self-healing of surface cracks in mortars with expansive additive and crystalline additive. Cement Concr Compos 2012;34:566–74.

[17] ACI Committee 212, 2010. Report ACI 212-3R-10, 2010. Report on chemical admixtures for concrete. American Concrete Institute (ACI), p 46–50.

[18] Jaroenratanapirom D, Sahamitmongkol R. Self-crack closing ability of mortar with different additives. J Met Mater Miner 2011;21:9–17.

[19] Ferrara L, Krelani V, Carsana M. A "fracture testing" based approach to assess crack healing of concrete with and without crystalline admixtures. Constr Build Mater 2014;68:535–51.

[20] Sisomphon K, Copuroglu O, Koenders EAB. Effect of exposure conditions on self healing behavior of strain hardening cementitious composites incorporating various cementitious materials. Constr Build Mater 2013;42:217–24.

[21] Desmettre C, Charron J-P. Novel water permeability device for reinforced concrete under load. Mater Struct 2011;44:1713–23.